Probabilistic Model for Low-Altitude Trapped-Proton Fluxes

M. A. Xapsos, *Senior Member, IEEE,* S. L. Huston, *Member, IEEE,* J. L. Barth, *Senior Member, IEEE,* and E. G. Stassinopoulos, *Senior Member, IEEE*

***Abstract*—A new approach is developed for the assessment of low-altitude trapped proton fluxes for future space missions. Low-altitude fluxes are dependent on solar activity levels due to the resulting heating and cooling of the upper atmosphere. However, solar activity levels cannot be accurately predicted far enough into the future to accommodate typical spacecraft mission planning. Thus, the approach suggested here is to evaluate the trapped proton flux as a function of confidence level for a given mission time period. This is possible because of a recent advance in trapped proton modeling that uses the solar 10.7-cm radio flux, a measure of solar cycle activity, to calculate trapped proton fluxes as a continuous function of time throughout the solar cycle. This trapped proton model [1], [2] is combined with a new statistical description of the 10.7-cm flux to obtain the probabilistic model for low-altitude trapped proton fluxes. Results for proton energies ranging from 1.5 to 81.3 MeV are examined as a function of time throughout solar cycle 22 for various orbits. For altitudes below 1000 km, fluxes are significantly higher and energy spectra are significantly harder than those predicted by the AP8 model.**

***Index Terms*—AP8, low earth orbit (LEO), probabilistic model, TPM-1, trapped protons.**

I. Introduction

TRAPPED proton fluxes are often the most important radiation consideration for spacecraft in low earth orbit. The AP8 trapped proton model [3] has provided useful information for many years and has been a de-facto standard for assessing trapped proton flux and dose. AP8 is a static global map of long-term average trapped proton flux. There are two versions of AP8–one for solar maximum and one for solar minimum conditions. They are based on selected satellite data that were measured in the 1960s and 1970s. As time has progressed, though, it has become apparent that there is a need for improved models based on more recent data in order to assess the feasibility of flying advanced technology microelectronics systems for future missions. For example, AP8 is only applicable to long-term missions. In addition, AP8 provides no information about the transition period between solar maximum and solar minimum conditions. In reality, the trapped fluxes vary continuously with time. Another factor is that AP8 does not indicate how much variation there can be from the expected long-term average values of trapped flux. An approach that accounts for these factors would be useful for limiting design margins and therefore design costs. Further discussion of the current shortcomings of AP8 can be found in a number of places [1], [2], [4], [5].

Recently, improvements have been made in models of low-altitude trapped protons. Analyses of data from the DMSP F7, CRRES, APEX, and SAMPEX spacecraft by AFRL, BIRA, and Aerospace Corporation have helped to update the base of data [6]–[9]. The Boeing Company developed a model that was initially based on the NOAA/TIROS satellite data from 1978 to 1995. A feature of this model is that it accounts for the evolution of trapped flux levels over the course of a solar cycle due to varying solar activity [1]. Another feature is that it incorporates the secular variation of the geomagnetic field so that the model can be applied over broad ranges of time. The Boeing model was thus a major advance in trapped proton models. The CRRES satellite data from 1990 to 1991 has now been added to this model to expand its spatial coverage up to near geosynchronous altitudes and to broaden its energy range to cover 1.5 to 81.3 MeV [2]. The model in its current form is now called the Trapped Proton Model-1 (TPM-1).

In this paper, a new statistical feature is added to TPM-1 to enhance its utility for long-term mission planning. There is currently little or no statistical information contained in trapped proton models [4], [6]. However, the trapped proton environment at low altitudes is variable from one solar cycle to the next, depending to a large extent on solar activity level. Higher activity levels heat up and expand the upper atmosphere, which increases the removal rate of trapped protons through collisional processes. This results in lower trapped proton fluxes during periods of higher solar activity.

One approach to planning future missions would be to use TPM-1 along with some assumption about future solar activity. However, solar activity levels are not reliably known very far into the future, especially when the period of interest is during a different solar cycle than the present one. More useful information could be provided to the spacecraft designer if fluxes could be calculated as a function of confidence level for a planned mission time period. Then the designer could more systematically balance the tradeoffs among risk, cost, and performance for the mission. That is the focus of this paper. In the following, a new statistical model of solar activity is added to TPM-1, based on solar 10.7-cm radio flux ($F_{10.7}$). $F_{10.7}$ is taken as a measure of solar activity, and a proxy for atmospheric heating in TPM-1. The model of $F_{10.7}$ describes its time-dependent variation over the course of a solar cycle and as a function of confidence level. These results are used with TPM-1 to calculate trapped proton

Manuscript received July 15, 2002; revised September 9, 2002. This work was supported by the NASA Marshall Space Flight Center Space Environments and Effects program.

M. A. Xapsos, J. L. Barth and E. G. Stassinopoulos are with NASA Goddard Space Flight Center, Greenbelt, MD 20771 USA (e-mail: Michael.Xapsos@gsfc.nasa.gov).

S. L. Huston is with The Boeing Company, Huntington Beach, CA 92647 USA.

Digital Object Identifier 10.1109/TNS.2002.805409

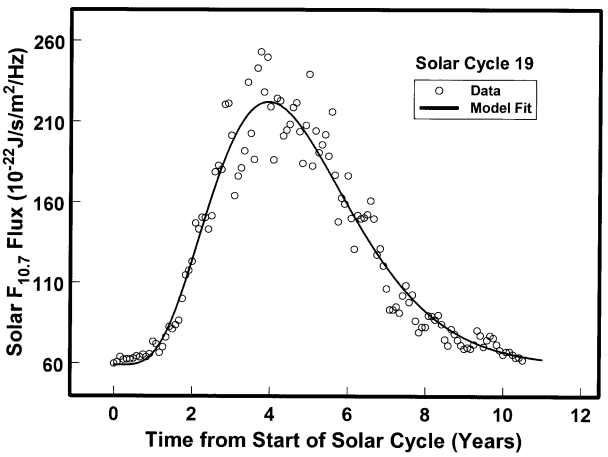

Fig. 1. $F_{10.7}$ as a function of time from the start of solar cycle 19. The data are obtained from the National Geophysical Data Center [10]. The line is the best fit of the statistical model.

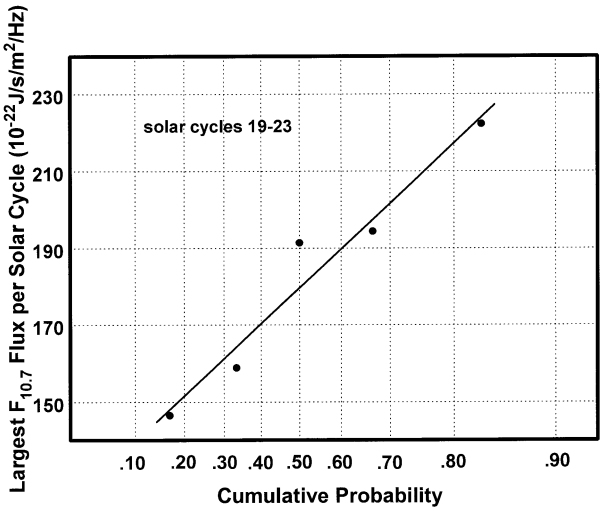

Fig. 2. Type I extreme value probability plot of the largest $F_{10.7}$ value in a solar cycle for cycles 19–23.

fluxes at given levels of confidence. This is the first rigorous probabilistic description of trapped proton fluxes.

II. Methods

A. TPM-1

TPM-1 is described in detail elsewhere [2]. Here we restrict ourselves to a brief description of how $F_{10.7}$ is used in this model. The proton flux for a given energy is related to $F_{10.7}$ through an empirical curve fitting procedure involving the geomagnetic coordinates and a phase delay in $F_{10.7}$. The phase delay corresponds physically to a time period associated with atmospheric expansion due to solar activity. Thus, TPM-1 uses a range of $F_{10.7}$ values as a function of time to calculate the trapped proton flux at a given location. TPM-1 currently contains historical $F_{10.7}$ data from April 1954 through August 2001 and projections up to January 2020. In this paper, the statistical model curves of $F_{10.7}$ for various confidence levels, described in the next section, were substituted for the standard $F_{10.7}$ values currently in the program.

B. Statistical Model for $F_{10.7}$

The data used for the probabilistic analysis of $F_{10.7}$ were obtained from the National Geophysical Data Center [10]. Measurements of $F_{10.7}$ have been made since 1947 during the descending phase of solar cycle 18. The data were the most refined values available. This includes corrections for antenna gain, atmospheric absorption, bursts in progress, background sky temperature, and the changing sun-earth distance. As an example, $F_{10.7}$ data for solar cycle 19 are shown by the points in Fig. 1. Mean monthly values are plotted as a function of time for the entire solar cycle. We have found that an empirical description of the data for each solar cycle (19 through the current cycle 23) is

$$f(t) = A \cdot g(t) + B. \tag{1}$$

This represents a time-dependent first term superimposed on a constant background, B. The constant A is a scale factor for the gamma density function, $g(t)$, which is given by [11]

$$g(t) = \frac{\nu(\nu \cdot t)^{k-1}}{\Gamma(k)} \exp(-\nu \cdot t). \tag{2}$$

Here ν and k are the parameters of the gamma density function and t is the time from the start of the solar cycle. The best fit of $f(t)$ to the data is shown by the curve in Fig. 1. It is seen that the fit describes the behavior of the $F_{10.7}$ data quite well. This is also true of $F_{10.7}$ for each solar cycle for which there is available data. The only parameters that it was necessary to vary from cycle to cycle for the fits were A and k. It turns out that these two parameters can be determined from the peak activity of a cycle. This will be very useful because the peak activity can be related to the confidence level. This is discussed next.

The peak value attained by a parameter representative of solar cycle activity is often used as an indicator of the overall activity level of the cycle [5]. Common examples of such parameters are $F_{10.7}$ and sunspot number. Thus, in order to assign confidence levels to solar cycle activities, a probability plot of the largest $F_{10.7}$ value observed in each of solar cycles 19–23 was constructed. The probability plot chosen was that of the type I extreme value distribution because the largest $F_{10.7}$ value of each cycle is of interest. These were obtained from fits such as that shown in Fig. 1 by determining the peak value of $f(t)$. The cumulative probabilities are equal to $m/(N+1)$, where m is the rank of the ordered data and N is the number of data points [12]. The probability plot is shown in Fig. 2. The applicability of the type I probability distribution to the data is determined by the data's linearity on the plot. Although the number of data points is somewhat limited, it is seen that they are well described by a straight line, indicating this is an appropriate distribution for describing the peak values of $F_{10.7}$. The maximum deviation of any point from the straight line is about 6%. Thus, the line in Fig. 2 relates $F_{10.7}$ to cumulative probability, which is equal to the confidence level.

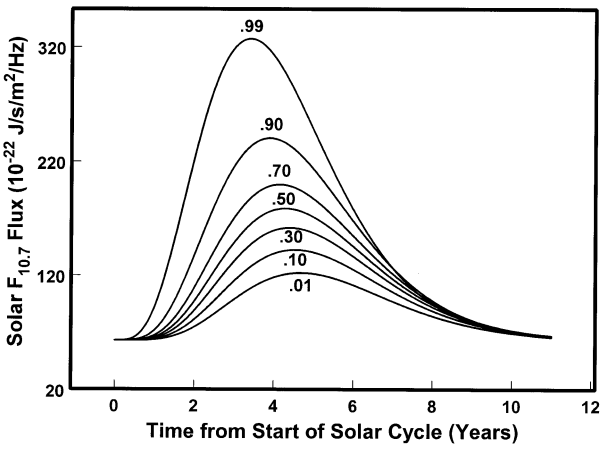

Fig. 3. Statistical model of $F_{10.7}$ as a function of time from the start of the solar cycle for confidence levels of 1, 10, 30, 50, 70, 90, and 99%.

The complete probabilistic description of $F_{10.7}$ can now be given. The only input required is to specify a confidence level for solar activity. The fitted line in Fig. 2 then gives the corresponding peak $F_{10.7}$ in the cycle. This determines the parameters A and k, whereas fitted values for B and ν are used that are always the same. Thus, $F_{10.7}$ can be calculated from (1) and (2) as a function of time for a specified confidence level. These results are shown in Fig. 3 for various levels of confidence. These statistical results reproduce the general observational trends for $F_{10.7}$. It is reasonably well established that the greater a cycle's activity, the faster the rise time to the peak level [13]. In all cases, $F_{10.7}$ starts off at a constant background level corresponding to the parameter B. More active cycles, i.e., those with greater peak activities, reach the peak levels earlier in the cycle. Similar to what is observed for sunspot numbers [14], the descending phase of the cycle is longer than the ascending phase. At the end of the cycle, $F_{10.7}$ returns to the same background level as at the cycle beginning. The interpretation of a confidence level of 90%, for example, is that a future solar cycle has a 90% probability of having an activity level that is less than or equal to that particular curve in Fig. 3.

III. Results

A. Solar Cycle Dependence

The results shown in Fig. 3 have been used as input files for TPM-1 in this work. Because we are concerned with heating and cooling effects in the upper atmosphere, our orbital considerations are limited to altitudes of less than 1000 km. The probabilistic trapped proton flux calculations are envisioned to be most useful when applied to future missions. However, for the purpose of comparing them to the standard TPM-1 results for validation purposes, calculations were done for the time period during solar cycle 22. As a first example, consider the original orbit of the International Space Station (ISS)–361-km perigee, 437-km apogee, and 51.6° angle of inclination. TPM-1 comes with an orbit generator, and this was used for these calculations. The filled circles in Fig. 4(a)–(c) show the time dependence of the omnidirectional differential trapped fluxes throughout solar cycle 22 calculated with the standard TPM-1. The proton energies shown are 10.7, 30.9, and 81.3 MeV in Fig. 4(a)–(c),

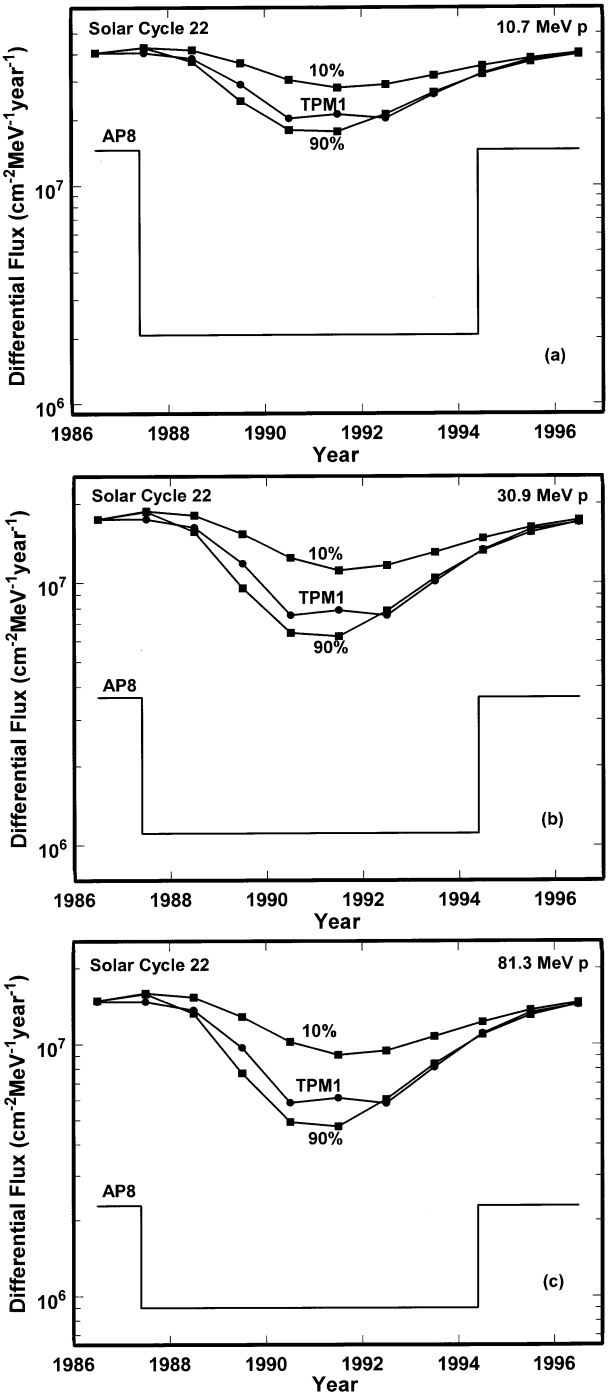

Fig. 4. Trapped proton differential flux for the original ISS orbit as a function of time during solar cycle 22. Shown are the standard results for TPM-1, results of the probabilistic model for 10% and 90% exceedance probabilities, and results for AP8. Proton energies are (a) 10.7 MeV, (b) 30.9 MeV, and (c) 81.3 MeV.

respectively. These are compared to the probabilistic trapped proton fluxes for 10% and 90% exceedance probabilities, shown by the squares. The interpretation of the 10% curve is that there is a 10% probability that the general trend of the flux levels in a given cycle will exceed it. Similarly, there is a 90% probability that the general trend of those flux levels in a given cycle will exceed that particular curve. Recall from previous discussion that higher levels of solar activity result in lower trapped proton

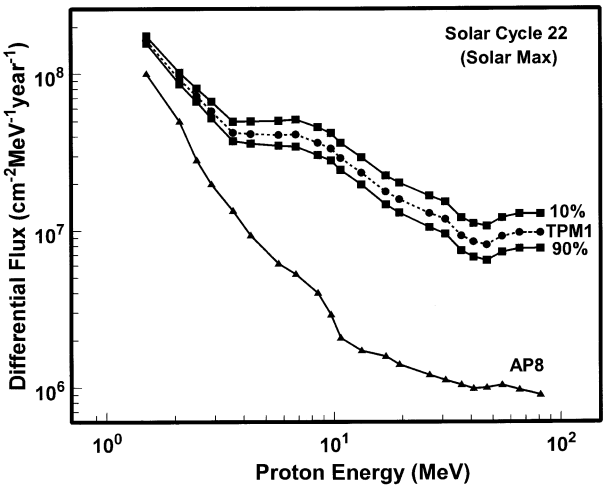

Fig. 5. Trapped proton energy spectra for the original ISS orbit in mid-year 1989 as calculated by the standard TPM-1, the probabilistic model, and AP8.

fluxes. The activity level of solar cycle 22 was quite high. In fact, in the last five cycles, its activity was exceeded only by that of cycle 19. Thus, the standard TPM-1 results for cycle 22 should fall much closer to the 90% curve than the 10% curve, and this turns out to be the case. An interesting feature of solar cycle 22 is the double-peaked behavior of its activity during solar maximum. The probabilistic model shown in Fig. 3 does not account for this type of detailed behavior. However, as seen in Fig. 4, it still does a reasonable job of bounding the fluxes even when a somewhat unusual feature such as this occurs.

Fig. 4 also shows comparisons to the AP8 model. The AP8 calculations were done with software developed by Armstrong and Colborn [15], and they were checked against AP8 results obtained using the CREME96 [16] and SPENVIS [17] web sites. The AP8 model provides only average flux values for solar minimum and for solar maximum conditions. Thus, there is the discontinuous behavior shown in the figures. The solar maximum period was assumed to be 7 years in duration, beginning 2.5 years before and ending 4.5 years after 1989 [14]. There are two significant points that should be made about the comparisons between TPM-1 and AP8. First, TPM-1 shows a more realistic, continuous transition between the solar maximum and solar minimum time periods. This feature will be especially useful for missions that occur during this transition phase. Second, the AP8 fluxes are significantly lower than the TPM-1 fluxes at these low altitudes. It is generally agreed that AP8 underestimates trapped proton fluxes at low altitudes, but it is not clear by how much. It has been reported that AP8 underestimates doses by about a factor of 2 at altitudes below 2000 km [18]. However, discrepancies in measured proton fluxes have been reported to be significantly greater than a factor of 2 at altitudes below 1000 km [1]. The flux differences reported here range from about a factor of 2 to 10. However, it must be kept in mind that dose measurements for such proton energy spectra are strongly influenced by the low-energy protons. It turns out that the flux differences reported here are not markedly inconsistent with previously reported low-altitude dose comparisons with AP8. In fact, Fig. 5 shows that the low-energy portion of the TPM-1 proton spectra exceeds AP8 fluxes by about a factor

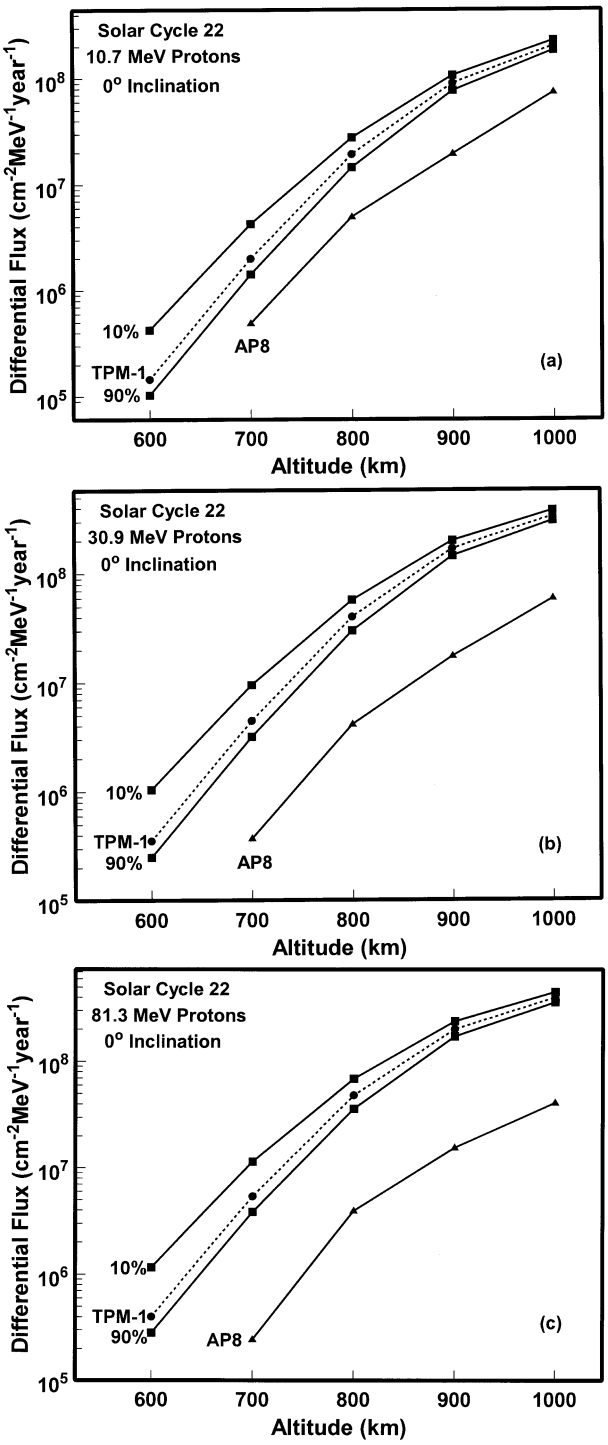

Fig. 6. Trapped proton differential flux as a function of orbital altitude in mid-year 1989 for a 0° inclination. Results are shown for the standard TPM-1, the probabilistic model for 10% and 90% exceedance probabilities, and AP8. Proton energies are (a) 10.7 MeV, (b) 30.9 MeV, and (c) 81.3 MeV.

of 2 for the above orbit. It is the higher energy fluxes where there are large differences between the two models. When comparing TPM-1 and AP8, another thing that must be considered is the instrumentation difference. The TPM-1 model is based primarily on the NOAA/TIROS satellite measurements, which are in reasonable agreement with both the low-altitude SAMPEX data [19] and the most reliable measurements made on CRRES,

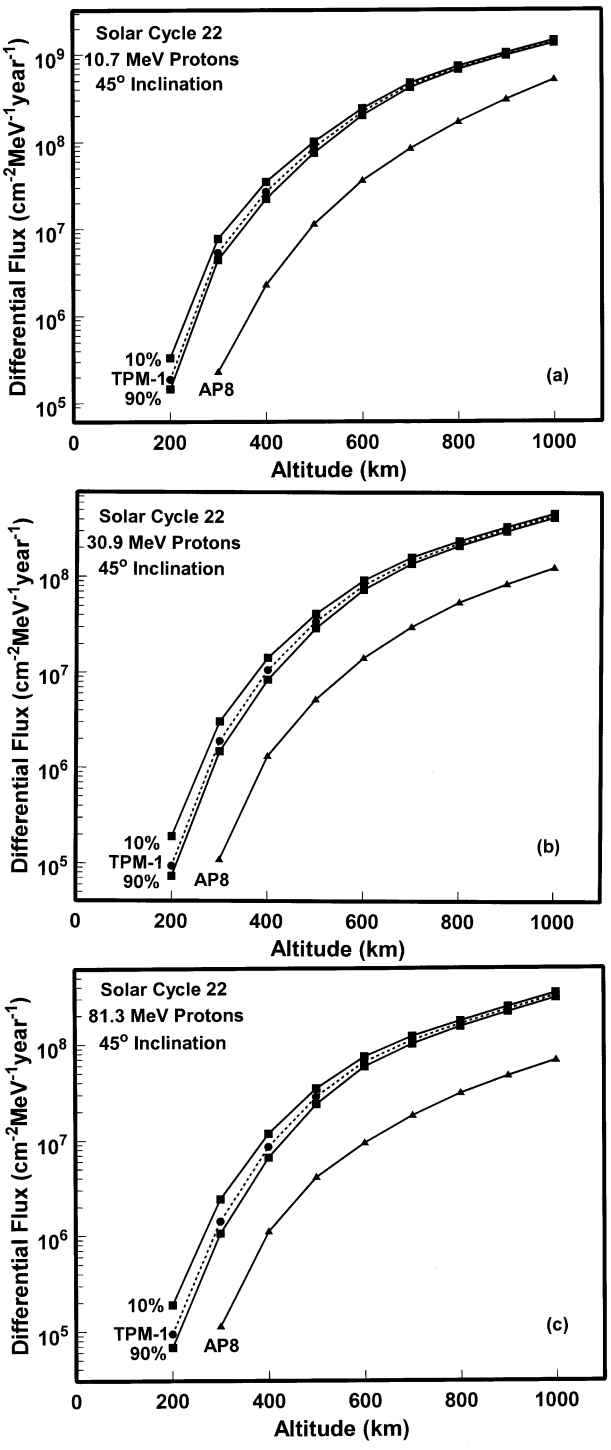

Fig. 7. Trapped proton differential flux as a function of orbital altitude in mid-year 1989 for a 45° inclination. Results are shown for the standard TPM-1, the probabilistic model for 10% and 90% exceedance probabilities, and AP8. Proton energies are (a) 10.7 MeV, (b) 30.9 MeV, and (c) 81.3 MeV.

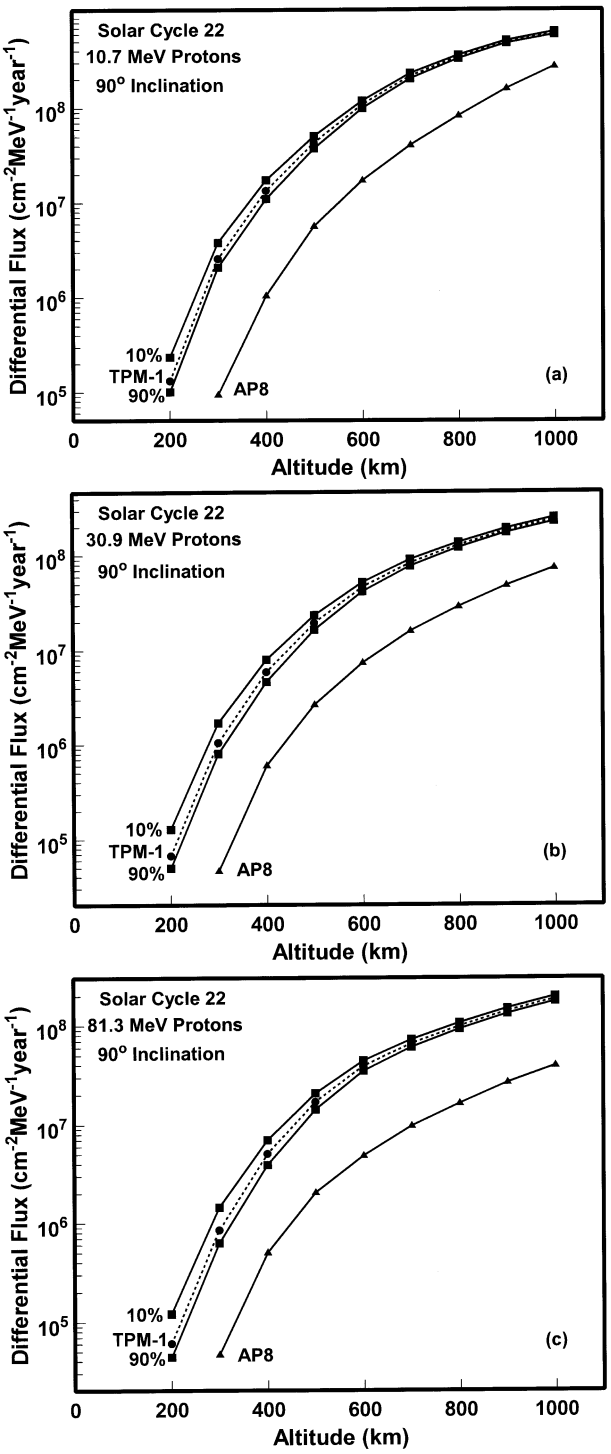

Fig. 8. Trapped proton differential flux as a function of orbital altitude in mid-year 1989 for a 90° inclination. Results are shown for the standard TPM-1, the probabilistic model for 10% and 90% exceedance probabilities, and AP8. Proton energies are (a) 10.7 MeV, (b) 30.9 MeV, and (c) 81.3 MeV.

which occurred at altitudes above 800 km [2]. The modern instrumentation used for these measurements is clearly an improvement over that used to collect data for AP8 in the 1960s and 1970s, and this must be considered when assessing the relative merit of the two models. On the other hand, TPM-1 is a model that is still in the developmental stages.

B. Energy Spectra

Fig. 5 shows the trapped proton differential energy spectra for the original ISS orbit at mid-year 1989, for energies ranging from 1.5 to 81.3 MeV. Again, the standard TPM-1 results are compared to the probabilistic results for 10% and 90% exceedance probabilities. Note that the spread in the probabilistic results is very small for low energies but reaches approximately

a factor of 2 at high energies. For many spacecraft applications, the high energies are the most important. The fact that the magnitude of this spread is similar to often quoted environmental uncertainties suggests that it is realistic to use the probabilistic approach for spacecraft design. For example, a 50% exceedance probability could be chosen to determine the average trapped proton flux. It could then be adjusted, presumably to a lower exceedance probability (higher flux) based on tradeoffs that the designer is willing to make.

Also shown in Fig. 5 is a comparison to the AP8 energy spectrum for solar maximum conditions. The TPM-1 model results show a harder energy spectrum. The two models are in reasonable agreement for proton energies around one or a few MeV but rapidly diverge at higher energies. At about 10 MeV and beyond, the flux differences are close to an order of magnitude. Similar results are seen for solar minimum conditions, although the differences with AP8 are not as pronounced [2].

C. Orbital Dependence

The magnitude and variability of the upper atmospheric expansion during solar maximum is an important consideration for low-altitude spacecraft. Thus, in this section, we examine how this affects the trapped proton flux as a function of altitude ranging from the atmospheric cutoff up to 1000 km. Fig. 6 shows calculations for an equatorial orbit at mid-year 1989. Differential fluxes of 10.7-, 30.9-, and 81.3-MeV protons are shown in Fig. 6(a)–(c), respectively. As is expected, the flux increases rapidly with increasing altitude. Also note that in a relative sense, the variability of the trapped flux decreases with increasing altitude. In fact, it turns out that for all cases studied here, the largest variability, about a factor of 4 between the 10% and 90% exceedance probabilities, occurs near the atmospheric cutoff in an equatorial orbit. Keep in mind that this variability represents a fluctuation in proton flux that can occur from one solar maximum time period to the next.

For comparison purposes, similar calculations were done for 45° and 90° inclination orbits. These results are shown in Figs. 7 and 8, respectively, and cover the same time period and proton energies as Fig. 6. In these orbits, the atmospheric cutoff is significantly lower–approximately 200 km. In addition, the flux variability is not as pronounced as for the equatorial orbit. In these higher inclination orbits, it is a factor of 2–3 at the lowest altitudes and decreases with increasing altitude. Finally, we again note the significant discrepancies with the AP8 model for proton fluxes above 10 MeV.

IV. Conclusion

This work suggests a new procedure for assessing the trapped proton environment for future low-altitude space missions. It is to evaluate trapped proton fluxes as a function of confidence level for the given mission time period. The advantage of this approach over conventional approaches is that it allows the spacecraft designer more flexibility to tradeoff cost, risk, and performance for the mission. This is important because conditions such as solar activity levels, which affect the low-altitude radiation environment, are not accurately known during the advanced mission planning period.

A confidence level model of solar activity was developed based on $F_{10.7}$ data. This was used with a new model of trapped proton flux, TPM-1, that features calculations of flux that are dependent on solar activity. Results indicated that the magnitude of the flux variations from one solar maximum time period to the next were consistent with commonly assumed environmental uncertainties, so that the confidence level approach would be practical to implement. The largest flux variations occur for low orbital altitudes and for low angles of orbital inclination. The flux variations also increase as the proton energy increases for the range of energies studied here. This confidence level approach further expands the utility of TPM-1.

References

[1] S. L. Huston and K. A. Pfitzer, "A new model for the low altitude trapped proton environment," *IEEE Trans. Nucl. Sci.*, vol. 45, pp. 2972–2978, Dec. 1998.

[2] S. L. Huston, "Space Environments and Effects: Trapped Proton Model," The Boeing Company, Huntington Beach, CA, NAS8-98 218, 2002.

[3] J. M. Sawyer and J. I. Vette, "AP8 Trapped Proton Model for Solar Maximum and Solar Minimum," National Space Science Data Center, Greenbelt, MD, NSSDC 76-06, 1976.

[4] E. J. Daly *et al.*, "Problems with models of the radiation belts," *IEEE Trans. Nucl. Sci.*, vol. 43, pp. 403–415, Apr. 1996.

[5] J. L. Barth, "Modeling space radiation environments," *IEEE Nuclear and Space Radiation Environment Conf. Short Course*, 1997.

[6] M. S. Gussenhoven, E. G. Mullen, and E. Holeman, "Radiation belt dynamics during solar minimum," *IEEE Trans. Nucl. Sci.*, vol. 36, pp. 2008–2014, Dec. 1989.

[7] J. D. Meffert and M. S. Gussenhoven, "CRRESPRO Documentation," Phillips Laboratory, Hanscom AFB, MA, PL-TR-94-2218, 1994.

[8] M. S. Gussenhoven, E. G. Miller, and E. Holeman, "APEXRAD: Low altitude orbit dose as a function of inclination, magnetic activity and solar cycle," *IEEE Trans. Nucl. Sci.*, vol. 44, pp. 2161–2168, Dec. 1997.

[9] D. Heynderickx *et al.*, "A low altitude trapped proton model for solar minimum conditions based on SAMPEX/PET data," *IEEE Trans. Nucl. Sci.*, vol. 46, pp. 1475–1480, Dec. 1999.

[10] [Online]. Available: ftp://ftp.ngdc.noaa.gov/STP/SOLAR_DATA/SOLAR_RADIO/FLUX/

[11] A. H.-S. Ang and W. H. Tang, *Probability Concepts in Engineering Planning and Design*. New York: Wiley, 1975, vol. I.

[12] E. J. Gumbel, *Statistics of Extremes*. New York: Columbia Univ., 1958.

[13] J. A. Joselyn *et al.*. Solar Cycle 23 Project: Summary of Panel Findings. [Online]. Available: http://www.sel.noaa.gov/info/Cycle23.html

[14] J. Feynman *et al.*, "New interplanetary proton fluence model," *J. Spacecraft*, vol. 27, pp. 403–410, 1990.

[15] T. W. Armstrong and B. L. Colborn, "TRAP/SEE Code Users Manual for Predicting Trapped Radiation Environments," Marshall Space Flight Center, MSFC, AL, NASA/CR-2000-209 879, 2000.

[16] [Online]. Available: http://crsp3.nrl.navy.mil/creme96/

[17] [Online]. Available: http://www.spenvis.oma.be/spenvis/

[18] T. W. Armstrong and B. L. Colborn, "Evaluation of Trapped Radiation Model Uncertainties for Spacecraft Design," Marshall Space Flight Center, MSFC, AL, NASA/CR-2000-210 072, 2000.

[19] D. Heynderickx, Private Communication, Belgisch Instituut voor Ruimte-Aeronomie (BIRA), Brussels, Belgium.